

Theory of Work-Function Change on Adsorption of Polarizable Ions

J. ROSS MACDONALD AND C. A. BARLOW, JR.

Texas Instruments Incorporated, P. O. Box 5936, Dallas, Texas

(Received 19 July 1965)

We first point out and correct an error which occurred in an earlier, more approximate theory of the work-function change accompanying ion adsorption. Next, certain of the approximations of this earlier work are lifted to produce a more accurate theory. In particular, the adsorbed ions and their images in the adsorbent are no longer approximated as ideal dipoles. We employ results of recent exact calculations to obtain quite accurate expressions for the electric fields due to these nonideal dipoles and thus for the induced polarization associated with these fields. Furthermore, the images of induced dipoles are explicitly taken into account in their effect upon the self-consistent depolarizing field. This approach leads to a new expression for the effective dielectric constant of the adsorbed phase which takes cognizance of discreteness effects. Theoretical predictions are found to be in agreement with data for Cs^+ and K^+ on tungsten for small θ and may apply well up to $\theta \gtrsim 0.6$. Finally we discuss possible explanations for the discrepancies near $\theta=1$.

INTRODUCTION

IN a previous paper¹ (to be termed I hereafter), we have considered the change in average work function of an electrically conducting adsorbent attendant upon the adsorption thereon of a monolayer or less of discrete, regularly arrayed particles. The adsorbent elements were assumed to be uncharged or charged and to exhibit any combination of a permanent dipole moment, induced dipolar polarization, and/or charge state of valence z_v . Imaging of discrete dipoles in the adsorbent was neglected except insofar as such imaging increased the effective polarizability or permanent dipole moment of each element. Imaging of adion charges was accounted for explicitly, however, but the resulting nonideal adion-image dipoles were approximated as ideal dipoles, as were any permanent or induced dipoles present.

A number of new expressions for work-function change, ΔV , were derived, and we believe those applying to adsorption of neutral species, such as adatoms or molecules, to be correct within the limitations of the approximations involved. We have discovered an unfortunate error in I, however, which makes incorrect the general results for adsorption of charged species. In the present work, we correct this error and compare the result with that of a much less approximate treatment in which the adion-image effective dipoles are not taken as ideal and the images of the dipoles induced in adions are explicitly accounted for. We initially restrict attention to polarizable adions without permanent multipole moments and consider only a grounded adsorbent electrode. The charge on the electrode q will then always be $-q_a$, where $q_a \equiv \theta N_s z_v e$ is the average charge density of adsorbed elements. Their maximum, or monolayer, surface concentration is taken as N_s ; thus θ is the fractional surface coverage and $0 \leq \theta \leq 1$.

If the zero of potential is taken at the electrode, then in the present case $\Delta V = -\psi_\infty$, where ψ_∞ is the potential at an "infinite" distance from the adsorbing surface.

Here "infinite" denotes a distance very large compared to r_1 , the nearest-neighbor spacing of discrete elements. For an adsorbent surface of finite extent, an "infinite" distance must also be small compared to the minimum linear extent of the adsorbed array of charge.

The above definitions ensure that ψ_∞ is the potential which would be obtained if all adsorbed charges and higher-order multipoles were smeared or spatially averaged in the adsorbent plane. The actual induced polarization which is present depends sensitively, however, on the discreteness of the adions and on the nonideal dipole structure of adion-image pairs. The difficulty in the calculation of ψ_∞ arises, therefore, in the self-consistent calculation of the induced polarization, taking depolarization effects into account.

CORRECTION OF PREVIOUS WORK

When adion polarizability α is negligible, the well-known result

$$\psi_\infty = \psi_\infty^0 \equiv 4\pi\theta N_s z_v e \beta \quad (1)$$

holds. Here β is the separation between the charge centroid of an adion and the imaging plane. When α is not negligible, we may write¹ for the induced polarization \mathcal{P}_1 ,

$$\mathcal{P}_1 = N_s \alpha \mathcal{E}_1 = \theta N_s \alpha \mathcal{E}_1 / d, \quad (2)$$

where N_s is the average number per unit volume of polarizable adions in the thickness d . Here

$$\mathcal{E}_1 \equiv \mathcal{E}_{n1} + \mathcal{E}_{\text{eff}}, \quad (3)$$

where \mathcal{E}_{n1} is an average "natural" field which may be present at the bare surface of the adsorbent.¹ The error in I arose from writing $\mathcal{E}_{\text{eff}} \equiv 4\pi q + \mathcal{E}_d$, where \mathcal{E}_d is a depolarizing field to be computed. Unfortunately, this innocuous expression counts the discrete charge twice, both in q and in \mathcal{E}_d . The correct formula is

$$\mathcal{E}_{\text{eff}} \equiv 4\pi(q + q_a) + \mathcal{E}_d. \quad (4)$$

Thus, in the present case where $q = -q_a$, $\mathcal{E}_{\text{eff}} = \mathcal{E}_d$. For adsorption of neutral entities $q_a \equiv 0$. In order to

¹ J. R. Macdonald and C. A. Barlow, Jr., *J. Chem. Phys.* **39**, 412 (1963); **40**, 237 (1964).

correct I, we must replace q by $(q+q_a)$ in the definition of ϵ_{eff} , in several obvious places on pp. 417 and 419, and in Eqs. (5), (13), (15)–(19), (26), (32), (34), and (35). In addition, the $4\pi\theta N_s \alpha z_v e / \epsilon_{\text{eff}}$ terms appearing in Eqs. (28) and (35) must be eliminated. Equation (28), which applies in the present case of polarizable adions, then leads to

$$\psi_\infty = -\Delta V = (4\pi\theta N_s / \epsilon) [\alpha \epsilon_{n1} + (2-\epsilon) z_v e \beta], \quad (5)$$

where for simplicity or added distinctivity of terms we have written ϵ for ϵ_{eff} , z_v for z , and β for d_1 . The effective dielectric constant ϵ remains the same and is, for a mobile, hexagonal array,¹

$$\epsilon \equiv 1 + \sigma(\alpha/\beta^3) R_1^{-3} \equiv 1 + b\theta^{\frac{3}{2}}, \quad (6)$$

where $R_1 \equiv r_1/\beta = R_{1m}\theta^{-\frac{1}{2}}$, R_{1m} is the minimum value of R_1 , $\sigma \cong 11.0341754$, and

$$b \equiv \sigma(\alpha/\beta^3) R_{1m}^{-3} \cong 8.894\alpha N_s^{\frac{1}{2}}, \quad (7)$$

since $N_s = (\frac{4}{3})^{\frac{1}{2}} r_{1m}^{-2} \cong 1.1547005\beta^{-2} R_{1m}^{-2}$.

Figure 1 shows how the normalized quantity $\Lambda \equiv \psi_\infty(\theta)/\psi_\infty^0(1)$ calculated using Eq. (5) with $\epsilon_{n1}=0$ depends on θ for various b values. A maximum is frequently observed experimentally in curves of this kind. Although Eq. (5) with $\epsilon_{n1}=0$ predicts a maximum at $\theta = \theta_m = \{[(13)^{\frac{1}{2}} - 3]/2b\}^{\frac{2}{3}}$, Fig. 1 shows that for θ_m to occur within the range of interest, b must be of the order of 0.4, or greater. This is usually greater than experimentally likely values of α and N_s lead to.¹ Further, Fig. 1 shows that Λ can even become negative in the range $0 \leq \theta \leq 1$ when $b > 1$. We have presented Fig. 1 in terms of θ variation for comparison with a similar (incorrect) figure in I. It turns out, however, that when the variable R_1^{-2} is used instead of θ , universal curves of ψ_∞ , suitably normalized, may be presented for different values of the single parameter $J \equiv \alpha/\beta$.³ Comparison on this basis of the predictions of Eq. (5) and those of a more accurate result will be presented later.

CALCULATIONS FOR NONIDEAL DIPOLES

In this section, we again take $(q+q_a)=0$. Further, since the earlier work included the case of polarizable adions having permanent dipole moments whose time-average component perpendicular to the adsorbent surface is $\langle \mu \rangle$, we treat this quite general case here as well. As usual, we make the excellent approximations that induced and permanent adion dipole moments are ideal, and we take them localized at the charge centroid of the adion.

From Gauss' law we have from Eq. (33) of I and from Eq. (2) of the present work,

$$\begin{aligned} \psi_\infty &= 4\pi q_a \beta + 4\pi \mathcal{O}_1 d + 4\pi \theta N_s \langle \mu(\mathcal{E}_2) \rangle \\ &= \psi_\infty^0 + 4\pi \theta N_s \alpha \mathcal{E}_1 + 4\pi \theta N_s \langle \mu(\mathcal{E}_2) \rangle, \end{aligned} \quad (8)$$

where \mathcal{E}_1 is defined in (3) and $\mathcal{E}_2 \cong \epsilon_{n2} + n^{-2}\epsilon_{\text{eff}}$, as discussed in I. Here n^2 is the square of the index of refraction of the ionic material being adsorbed, and

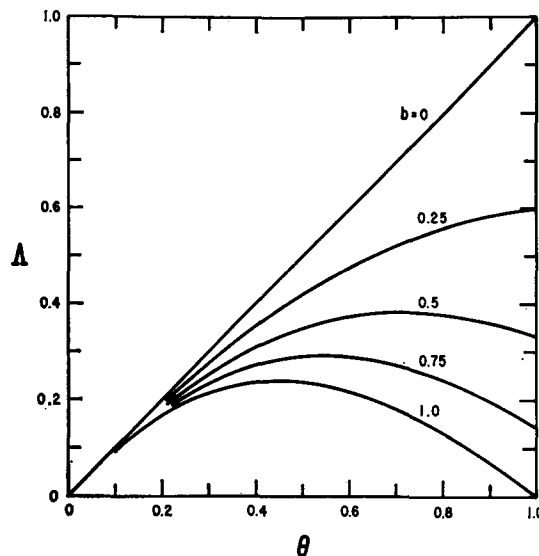


FIG. 1. Dependence of $\Lambda \equiv \psi_\infty(\theta)/\psi_\infty^0(1)$ on θ for various b values. Calculations based on Eq. (5) with $\epsilon_{n1}=0$.

ϵ_{n2} is an orienting natural surface field which may possibly differ from ϵ_{n1} . Notice that Eq. (8) involves average quantities as it should; nevertheless, discreteness effects are of great importance in determining the actual amount of average induced polarization and permanent dipole orientation. Their influence must therefore be properly included in the determination of ϵ_{eff} and \mathcal{E}_d .

Consider an infinite, plane, hexagonal array of adsorbed elements. Remove one element completely, keeping the position, polarization, average permanent dipole orientation, and charge of all surrounding elements and their images (including the charge and dipole images of the removed element) fixed and at their original values. Then \mathcal{E}_d is the field acting at the (vacant) position of the charge centroid of the removed element (a perpendicular distance of β from the electrode) before it was removed. It is through this depolarization field that discreteness effects make themselves felt. It is here termed a depolarizing field because its major parts tend to polarize the adions in the direction opposite to that of the nonideal dipoles formed by adion charges, $z_v e$, and their images.

There are five logically separate additive contributions to \mathcal{E}_d which we identify as \mathcal{E}_{di} , $i=1, 2, 3, 4, 5$. First there are the contributions arising from the image charge \mathcal{E}_{d1} and image dipoles (permanent and induced) \mathcal{E}_{d2} of the single removed adion. These are

$$\mathcal{E}_{d1} = -z_v e / 4\beta^2, \quad (9)$$

$$\mathcal{E}_{d2} = [\alpha \mathcal{E}_1 + \langle \mu(\mathcal{E}_2) \rangle] / 4\beta^3. \quad (10)$$

Next come the contributions from all other surrounding, real induced and permanent (ideal) dipoles. From I, these are

$$\mathcal{E}_{d3} = -[\alpha \mathcal{E}_1 + \langle \mu(\mathcal{E}_2) \rangle] \sigma r_1^{-3}. \quad (11)$$

Here, we have replaced an infinite lattice sum by its value σr_1^{-3} , where again $\sigma \cong 11.0341754$ for a hexagonal array.^{2,3}

The field terms \mathcal{E}_{d4} and \mathcal{E}_{d5} arise, respectively, from all surrounding nonideal dipoles formed by the adion charges and their images and from the images of all surrounding ideal dipoles. We find and use approximate but quite accurate expressions for these two contributions.

We have recently completed a rather involved but very accurate calculation of fields and potentials anywhere in front of a plane electrode on which is adsorbed and imaged an infinite hexagonal array of nonpolarizable adions, or monopoles.⁴ On comparison of these results with the predictions of an approximate "cutoff" model of the situation introduced by Grahame,⁵ we have found that a parameter r_0 in this model can be selected such that values of fields and potentials calculated from this simple model are correct to within several percent over the entire range of θ or R_1 of interest. We use this model, with slight further modification which increases its accuracy appreciably, for \mathcal{E}_{d4} and \mathcal{E}_{d5} . By this artifice, we avoid the need to use the very complicated formulas of the nonideal dipole treatment mentioned above while still ensuring high accuracy in simple expressions for \mathcal{E}_{d4} and \mathcal{E}_{d5} .

The cutoff model for nonideal dipoles smears the discrete adion and image charges in their planes and replaces them by uniform charge sheets (having the same average charge density as the discrete distribution) with colinear circular vacancies each having a radius r_0 . Grahame took $r_0 = (\pi\theta N_e)^{-1} \cong 0.5250376 r_1 \cong r_1/1.90463$. We instead use $r_0 = 4\pi r_1/\sqrt{3}\sigma \cong r_1/1.520865$, a value which allows the cutoff model to agree exactly with a model based on ideal dipoles [see, e.g., Eq. (11)] in the limit $R_1 \rightarrow \infty$. In this limit, nonideal dipoles can be treated as ideal; thus, the cutoff model with the above r_0 gives correct results in this limit. With no further modification, the cutoff model yields an expression for, e.g., \mathcal{E}_{d4} , correct over the R_1 range from 0.1 to ∞ to within a few percent.

It turns out that the cutoff model for fields of interest herein involves terms like $[1 + (2\pi R_1/\sqrt{3}\sigma)^2]$. We have found that considerable added accuracy can be obtained if we write instead $[\mathcal{p} + (2\pi R_1/\sqrt{3}\sigma)^2]$ and determine \mathcal{p} by nonlinear least-squares fitting of accurate field data. Whatever the value of \mathcal{p} resulting, the correct limiting behavior for $R_1 \rightarrow \infty$ will still be maintained, while the use of such a best \mathcal{p} can reduce errors appreciably for smaller R_1 values. Using the expression for \mathcal{E}_{d4} which follows from our earlier work on the cutoff model,⁴ modified by replacing 1 by \mathcal{p} , we find $\mathcal{p} = 0.9117$. In the main range of interest, $1 \leq R < \infty$ the largest error

in the predicted normalized quantity $\beta \mathcal{E}_{d4}/\psi_\infty^0$ is less than 0.006. The resulting simple expression for \mathcal{E}_{d4} is

$$\mathcal{E}_{d4} = -(\psi_\infty^0/2\beta) [0.9117 + (2\pi R_1/\sqrt{3}\sigma)^2]^{-1/2}. \quad (12)$$

In obtaining \mathcal{E}_{d3} , we used a lattice sum first evaluated by Topping.² It gave the field in the plane of a hexagonal array of discrete ideal dipoles. Unfortunately, this sum cannot be used in determining \mathcal{E}_{d5} because here we require the field at a distance 2β in front of an ideal dipole image array with the central dipole missing. We can, however, use the cutoff model by replacing the discrete, ideal dipoles by a single smeared dipole sheet with a central circular hole of radius $r_0 = 4\pi r_1/\sqrt{3}\sigma$ in it. Direct evaluation of the field for this situation or letting the separation of the charge pairs in the nonideal dipole cutoff model go to zero and evaluation of the field at a distance 2β in front of the plane both yield

$$\mathcal{E}_{d5} = -\left(\frac{8\pi^3}{3^3\sigma^2}\right) \left[\frac{\alpha \mathcal{E}_1 + \langle \mu(\mathcal{E}_2) \rangle}{\beta^3} \right] \left[1 + \left(\frac{2\pi R_1}{\sqrt{3}\sigma}\right)^2 \right]^{-1/2}. \quad (13)$$

Since we are here dealing with an array of ideal dipoles already and \mathcal{E}_{d5} itself leads to only a small correction term, we have not used \mathcal{p} in (13) instead of 1.

Let us now combine Eqs. (3) and (4), form and use \mathcal{E}_d , and finally solve for \mathcal{E}_1 . The result may be written

$$\mathcal{E}_1 = [\mathcal{E}_3 + \mathcal{E}_4 + \mathcal{E}_{d4}]/\epsilon_1, \quad (14)$$

where now

$$\mathcal{E}_3 \equiv \mathcal{E}_{n1} - (z_0 e/4\beta^2), \quad (15)$$

$$\mathcal{E}_4 \equiv [\alpha^{-1}(1 - \epsilon_1)] \langle \mu(\mathcal{E}_2) \rangle, \quad (16)$$

and

$$\epsilon_1 \equiv 1 + (\alpha/\beta^3) \{ \sigma R_1^{-3} - \frac{1}{4} + (8\pi^3/3^3\sigma^2) [1 + (2\pi R_1/\sqrt{3}\sigma)^2]^{-1/2} \}. \quad (17)$$

The new effective dielectric constant ϵ_1 incorporates the terms appearing in the earlier, more approximate ϵ but also includes new terms arising from the image of the charge of a single ion and the ideal dipole image layer. Note that as $R_1 \rightarrow \infty$, the last R_1 term in (17) goes to σR_1^{-3} , equal to the first term in the braces. In this limit

$$\epsilon_1 \rightarrow 1 - (\alpha/4\beta^3).$$

Finally, the combination of Eqs. (2), (8), and (14) yields ψ_∞ . Note, however, that \mathcal{E}_2 also involves \mathcal{E}_1 ; thus, \mathcal{E}_1 still occurs on both sides of (14) through $\langle \mu(\mathcal{E}_2) \rangle$. In the absence of an explicit form for the dependence of $\langle \mu \rangle$ on \mathcal{E}_2 , this is as far as we can go.

To obtain an explicit result superior to the present Eq. (5), we now consider only polarizable adions without permanent dipole moments. Then $\mathcal{E}_4 \equiv 0$, and ψ_∞ may be written

$$\begin{aligned} \psi_\infty &= \psi_\infty^0 [1 + (\alpha \mathcal{E}_1/z_0 e \beta)] \\ &\equiv \psi_\infty^0 [1 - g(R_1)], \end{aligned} \quad (18)$$

² J. Topping, Proc. Roy. Soc. (London) **A114**, 67 (1927).

³ B. M. E. van der Hoff and G. C. Benson, Can. J. Phys. **31**, 1087 (1953).

⁴ C. A. Barlow, Jr., and J. R. Macdonald, J. Chem. Phys. (to be published).

⁵ D. C. Grahame, Z. Elektrochem. **62**, 264 (1958).

where

$$g(R_1) = \frac{1}{2\epsilon_1} \left(\frac{\alpha}{\beta^3} \right) \left[\frac{(8\pi/\sqrt{3}) R_1^{-2}}{[0.9117 + (2\pi R_1/\sqrt{3}\sigma)^2]^{\frac{1}{2}}} + \frac{1}{2} - 2 \left(\frac{\beta}{z_v e} \right) (\beta \epsilon_{n1}) \right] \quad (19)$$

Comparison of (5) and (18) shows that although they both go to zero as $\theta \rightarrow 0 (R_1 \rightarrow \infty)$, they are appreciably different for finite θ . Omitting the single image charge term in (18), we find that (5) and (18) approach the same form as $\theta \rightarrow 0$. They are still not exactly the same, however, since one involves ϵ and the other the different ϵ_1 in place of ϵ .

In I we mentioned that imaging of the ideal dipoles associated with adion-induced polarization could be accounted for approximately by an (R_1 -independent) increase in α . Our present results show how the actual increase depends on R_1 . The quantity α/ϵ_1 occurs in Eq. (19), and the effect of the above imaging is included in the last two terms of ϵ_1 . It turns out that for $R_1 \geq 2$, and thus in the range of interest, the sum of these terms is negative, decreasing ϵ_1 and increasing the effective α . The largest relative increase occurs at $R_1 = \infty$, where α/ϵ_1 becomes

$$\frac{\alpha}{[1 - (\alpha/4\beta^3)]}$$

Even this increase will usually be quite small for adions with their small polarizability.

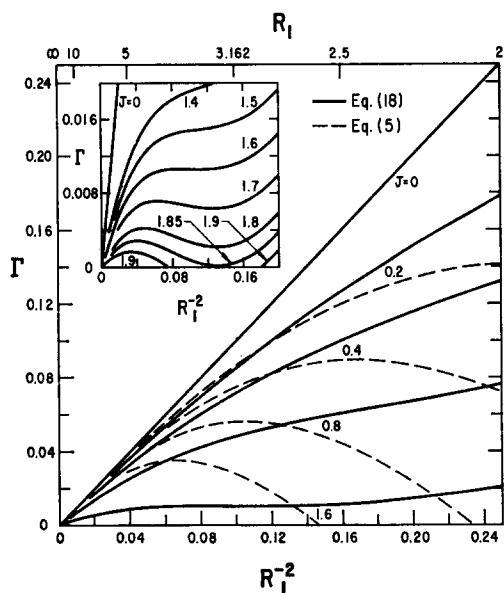


FIG. 2. Dependence of $\Gamma \equiv \psi_\infty / (\psi_\infty^0)_{R_1=1}$ on R_1^{-2} for various $J = \alpha/\beta^3$ values. Comparison of approximate Eq. (5) results (solid lines), and more accurate Eq. (18) predictions (broken lines). Inset shows behavior of Eq. (18) for J approaching 2; note changed scales.

TABLE I. Parameters determined by least-squares curve fitting.

System	H (V)	J	R_{1m}	S
Cs on W	54.38	1.836	4.063	0
	49.37	2.499	4.937	0.25
K on W	23.25	1.705	4	0
	100.2	1.948	6.179	0

Figure 2 shows $\Gamma \equiv \psi_\infty / (\psi_\infty^0)_{R_1=1} \equiv \psi_\infty / HR_{1m}^{-2}$ versus R_1^{-2} . Here

$$H \equiv \psi_\infty^0 / \theta \equiv (8\pi/\sqrt{3}) (z_v e / \beta) R_{1m}^{-2} \cong 208.93 z_v R_{1m}^{-2} \beta^{-1} \text{ V,}$$

where β is in angstroms in the last form. We use a R_1^{-2} scale because R_1^{-2} is proportional to θ ; yet the transformation constant, R_{1m} , does not enter the calculations. The R_1^{-2} scale can be converted to a θ scale by multiplying by R_{1m}^2 . The top of Fig. 2 shows a few values of R_1 itself. We have again neglected ϵ_{n1} in Eqs. (5) and (18); even a magnitude as large as 10^7 V/cm leads to negligible contribution from the ϵ_{n1} term for reasonable values of β .

We see from Fig. 2 that there is considerable difference between the predictions of Eq. (5) and those of the less approximate Eq. (18). Note especially also that (18) predicts no maximum in ψ_∞ until $J \lesssim 1.6$ and that in this range the maximum magnitude of Γ is greatly reduced. Another difference is that the initial slope, $m \equiv (\psi_\infty/\theta)_{\theta=0}$, associated with Eq. (5) is just H , independent of J , while that following from (18) is $m = \{[4 - 2J(1 - S)] / (4 - J)\} H$. Here we have written S for $2(\beta/z_v e) (\beta \epsilon_{n1}) \cong (1.389/z_v) \beta^2 \epsilon_{n1} \times 10^{-9}$, where β is in angstroms in the last form and ϵ_{n1} in volts per centimeter. As shown by the inset in Fig. 2, this initial slope with $S=0$ is much less than H when J is near 2.

We have fitted Eq. (18) to $\psi_\infty(\theta)$ data for cesium⁶ and potassium⁷ on tungsten by using nonlinear regression to obtain least-squares values for the parameters H , J , R_{1m} , and S . Some of the results are shown in Table I. In the instances shown, S was initially fixed and the other parameters determined. It was found, however, that when S also was permitted to vary during regression iteration, there was essentially no change in it or the other parameters, provided the initial values for the iteration were those obtained with S fixed, including the given value of S . Therefore, we have not shown such results obtained with all the parameters variable since they differ inappreciably from those given. Note that $S = \frac{1}{4}$ corresponds to ϵ_{n1} of about 8×10^7 V/cm when $z_v = 1$ and $\beta = 1.5$ Å. Even with adions nestling down somewhat between adsorbent surface atoms, electron overlap would probably not lead to a field at the adion center this large.

Although an excellent fit of the data could be obtained with any physically likely value of S , this was luckily

⁶ J. B. Taylor and I. Langmuir, Phys. Rev. **44**, 423 (1933).

⁷ L. Schmidt and R. Gomer, J. Chem. Phys. **42**, 3573 (1965).

not found to be the case for the other parameters. For example, in the fitting resulting in the next to last row of Table I, S was held fixed at 0 and R_{1m} at 4. A considerably poorer fit of the data was obtained than when R_{1m} was left free to vary, as in the last row.

It is noted that good fits required large values of H and J values relatively near 2. Unfortunately, these values do not lead to reasonable magnitudes for such quantities as β , r_{1m} , and α . For example, if we take $z_v = 1$, the top H and R_{1m} values for Cs in Table I lead to $\beta \approx 0.23 \text{ \AA}$, much smaller than seems likely.^{1,8} For $z_v < 1$, β would be even smaller. In turn, this value of β and $J = 1.836$ leads to $\alpha \approx 0.02 \text{ \AA}^3$, about 100 times smaller than that likely for Cs⁺. Finally, this value of β and $R_{1m} = 4.063$ leads to a value of N_s more than 20 times larger than possible. Similar impossibilities arise from analysis of the K⁺ results.

The above results indicate that equations such as (18) should not be applied to fit data over the entire θ range. First, there is usually some uncertainty in establishing from experiment the θ scale and the $\theta = 1$ point. If the scale were incorrect by a constant scale factor, values of R_{1m} such as those in Table I would also be incorrect. Some of this uncertainty could be eliminated if experimentalists used a scale based on the measured number density of adsorbed particles. Determining this density would still require a knowledge on the part of the experimentalist of the true surface area. If the surface were not truly planar, this area would exceed the apparent area of the adsorbing surface and estimates of r_1 would be too small. Note, however, that, provided the surface is nearly planar over distances large compared with the separation r_1 and given the correct value of r_1 , the present theory applies well even though the surface may be rough on a larger scale. Another uncertainty arises because there is a possibility that for many systems $z_v < 1$ and that z_v may even be a function of R_1 . Finally, it seems likely that irrespective of whether the appropriate effective z_v is < 1 and/or varies with θ the adsorbed particles may be a θ and temperature-dependent sum of adions and adatoms. At usual experimental temperatures the particles are probably all ions for small θ , but there may be a majority of adatoms for θ near unity.⁸⁻¹⁰

⁸ J. A. Becker, *Advan. Catalysis* **7**, 135 (1955).

⁹ J. W. Gadzuk, Quarterly Progress Report No. 72, MIT 15 January 1964, pp. 170-171. See also J. W. Gadzuk, M.S. thesis, Department of Mechanical Engineering, MIT 15 January 1965.

¹⁰ N. S. Rasor and C. Warner, *J. Appl. Phys.* **35**, 2589 (1964).

Such effects as possible variable z_v and an increasing proportion of adatoms may make it inappropriate to fit entire experimental $\psi_\infty(\theta)$ curves with an equation for adions alone such as (18).

On the other hand, (18) should apply better than any earlier equations for small θ on the reasonable assumptions that z_v is constant in this range and no adatoms are present. In particular, the initial slope of $\psi_\infty(\theta)$ curves should be fitted by the combination of J , H , and S given above. As an example, take⁸ $m = 5.5 \text{ V}$ for Cs⁺ on W. The minimum value of r_1 is apparently about twice the diameter of a tungsten atom,^{1,6,8} or 5.48 \AA . If $R_{1m} = 4$, then $\beta \approx 1.37 \text{ \AA}$, a reasonable value if the adions sit down somewhat between surface tungsten atoms.^{1,8} If this effect is not too great, the deviation of the imaging surface from an ideal plane will not affect the present formulas appreciably. Taking $z_v = 1$ in addition, we calculate $H \approx 9.53 \text{ V}$. From this, the neglect of S compared to unity, and $m = 5.5 \text{ V} = [(4 - 2J)/(4 - J)]H$, we find $J \approx 1.19$. This result, together with $\beta \approx 1.37 \text{ \AA}$, finally leads to $\alpha \approx 3.05 \text{ \AA}^3$, not far from the usually quoted^{1,6} value of 2.46 \AA^3 and less than the value 3.14 \AA^3 given by Tessman, Kahn, and Shockley.¹¹ Although the α value obtained in this fashion is reasonable, note that it depends strongly on the value of β used, and this value is itself somewhat uncertain. Nevertheless, the experimental value of m is explained with reasonable values of the parameters and without the necessity of taking $z_v < 1$, as is sometimes done.⁷ Finally, a good fit of $\psi_\infty(\theta)$ data for $0 \leq \theta \lesssim 0.6$ may be obtained using Eq. (18) and physically reasonable values of all the parameters. It is only when the regression analysis is extended over the entire θ range that physically unlikely values of some of the parameters appear. Although the foregoing analysis demonstrates the possibility that $z_v \approx 1$ for $\theta \lesssim 0.6$, the case $z_v \neq 1$ cannot be ruled out insofar as reasonable fits are also obtainable in this situation as well. Accordingly, and in view of recent experiments and analysis by Utsugi and Gomer¹² which seem to support the supposition $z_v = 0$ even for small θ , we regard the parameters obtained from $z_v = 1$ fitting as reasonable, though possibly rough, estimates of the true values for Cs on W. The $z_v = 0$ conclusion is, however, open to question because depolarization fields were apparently neglected in the comparison¹² of the $z_v = 0$ and $z_v \neq 0$ cases.

¹¹ J. R. Tessman, A. H. Kahn, and W. Shockley, *Phys. Rev.* **92**, 890 (1953).

¹² H. Utsugi and R. Gomer, *J. Chem. Phys.* **37**, 1720 (1962).